# Modeling and Validation of Precipitate Formation During the Heat Treatment of 50CrMo4 Steel

Abigail Austin[1,2], Dr. Hermann Autenrieth[1], Dr. Stefan Dietrich[2], Prof. Dr. rer. nat. habil. Astrid Pundt[2] and Prof. Dr.-Ing. habil. Volker Schulze[2]

[1]*Robert Bosch GmbH, Center for Research and Advanced Engineering, 71272 Renningen, Germany*
[2]*Institute for Applied Materials – Materials Science and Engineering, Karlsruhe Institute of Technology, 76131 Karlsruhe, Germany*

In the manufacture of steel products, heat treatment plays an influential role in the properties of the steel. During this process, several changes at the microstructure level take place to help achieve the desired properties. One such occurrence is the nucleation, growth, and coarsening of precipitates. Factors such as temperature and time can affect the type of precipitate, its shape, size, number density etc. in the microstructure. These in turn affect the final mechanical properties. Knowledge of the precipitates formed can be a strategic step in further understanding the microstructure behavior and optimizing the heat treatment parameters.

This study focuses on 50CrMo4 martensitic steel with carbide precipitation. 50CrMo4 was subjected to range of tempering process parameters i.e., varying tempering temperatures and times. Carrying out detailed experiments to analyze the carbides over a wide range of process parameters is time-consuming and costly. In this case, a physics-based model of the precipitation is sensible to predict the behavior of the metal under a particular heat treatment process. A modelling approach such as JMA (Johnson-Mehl-Avrami) was used to determine parameters like the volume fraction of the carbides during isothermal holding while tempering. Other parameters, such as the number density and the size of the carbides, were also modelled to give a complete picture of precipitate formation. The kinetics of the carbides was successfully determined through modelling for tempering time ranging from a few seconds to hours.

Scanning and transmission electron microscopy investigations coupled with image analysis provide experimental data for the carbides in the heat-treated specimens. The physics-based model results are validated using these experimental data. The model results are in accordance with the experimental results. The physics-based model combined with the available experimental data can provide results with increased accuracy. This prediction model provides an additional level of insight into the behavior of 50CrMo4 steel and the necessary heat treatment parameters.

***Keywords:*** *precipitation kinetics, carbides, quenched and tempered steel, 50CrMo4, SAE 4150, electron microscopy*

## 1. Introduction

Quenched and tempered 50CrMo4 (SAE 4150) steel has a wide application range and its major form of failure is by fatigue [1]. Multiple studies indicated the influence of the precipitates on the mechanical properties of steel. The variations in heat treatment parameters influence the size, shape, distribution of the carbides which in turn affects the yield strength, toughness, notch impact energy, strain hardening etc. [2, 3, 4]. Studies also show the effect of other alloying elements on the formation of precipitates. For eg. Cr, Mo slows the coarsening of cementite [5]. This indicates that knowledge of the precipitates formed can be beneficial to manufacturing an optimal end usage application.

The precipitates formed in the steel can be evaluated by experimental approaches like electron microscopy, atom probe tomography (APT), X-ray diffraction (XRD), Selected area diffraction (SAD), energy dispersive X-ray spectroscopy (EDXS) [6, 7]. These approaches give information regarding the shape, size, count, location, chemical composition, crystallographic structure of precipitates. This enables a complete microstructure characterization, though time consuming and expensive.

Modeling of the precipitates has been a topic of study for decades. It can be broadly classified into microscopic, mesoscopic, and atomic scales with approaches like Kampmann-Wagner numerical (KWN), phase field modeling, Monte Carlo respectively [8]. This study focuses on the microscopic scale. The Johnson-Mehl-Avami (JMA) approach characterizes the phase transformation kinetics with a single parameter, the volume fraction. Modifications to the JMA accommodates the multiple-phase precipitations [9, 10]. Various nucleation, growth, and coarsening models have been implemented, as seen in studies such as [11, 12, 13]. Several precipitation simulation software packages are also available: MatCalc, TC-Prisma, JMatPro etc.

In the present study, SEM and TEM investigations of furnace heat treated 50CrMo4 steel specimens are performed for microstructure characterization. On the other hand, the precipitation kinetics showing the volume fraction of the carbides is modeled using JMA approach. The results show the comparison between experimental and modeling approaches. Both the outputs agree for most cases. A larger scatter is seen in the experimental results.

## 2. Experiment

### 2.1 Heat Treatment

In this work, low alloy 50CrMo4 (SAE 4150) steel is used. The chemical composition mentioned in Table 1 [14]. The experimental investigations focus on furnace heat-treated unnotched fatigue specimens with dimensions illustrated in Figure 1. The samples were austenitized at 850 °C for 20 min, followed by quenching in a Nitrogen medium. Subsequently, the specimens were subjected to tempering at 300 °C, 400 °C or 600 °C for durations of 2 hours or 6 hours, followed by cooling in a Nitrogen medium.

Table 1 Chemical composition of 50CrMo4 in wt%. [14]

| *C* | *Si* | *Mn* | *P* | *S* | *Cr* | *Mo* | *Fe* |
|---|---|---|---|---|---|---|---|
| 0.52 | 0.26 | 0.74 | 0.014 | 0.008 | 1.31 | 0.18 | Bal |

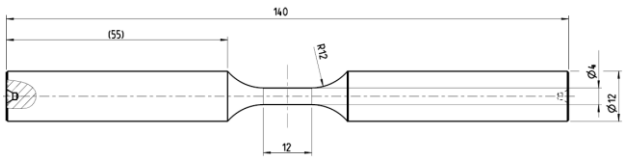

Figure 1 Specimen geometry.

### 2.2 Microstructure Characterization

The microstructure investigations employed scanning electron microscopy (SEM) and transmission electron microscopy (TEM) techniques. The central portion of the heat-treated specimen, with the dimension of Φ 4 mm, was cut out and prepared for the same. Imaging took place on the circular cross-section located at the center of the specimen. For SEM evaluation, the samples were ground, polished, etched with 1% Nital and investigated using Zeiss UltraPlus. TEM foils were prepared from polished samples using the Focused Ion Beam (FIB) method with FEI Strata 400S. TEM analysis was obtained from Philips CM 200 FEG/ST. This is combined with Scanning TEM (STEM) EDXS conducted with FEI Osiris ChemiStem. Image processing software Fiji [15] facilitated the assessment of the visible precipitates from the SEM and TEM analysis.

## 3. Theory

### 3.1 Johnson-Mehl-Avrami

This work focused on modeling the precipitation kinetics during the isothermal tempering process. The JMA approach is used to describe the phase transformation and hence insight into the volume fraction of the carbides. For the chosen low alloy steel, transition ε-carbide and cementite precipitates are considered in the modelling. The volume fraction of cementite based on JMA is as follows [10].

$$V_\theta = V_{\theta,max}*(1 - \exp\{-(\beta_\theta)\wedge n_\theta\})$$

Considering an isothermal tempering case:

$$\beta_\theta(t) = K_{0,\theta} \int \exp(-Q_\theta/(R*T(t))\, dt$$

with integration from 0 to $t$

where,

- $\theta$: Values for cementite
- $V_{\theta,max}$: Max volume fraction
- $n_\theta$: Avrami exponent
- $\beta_\theta$: State coefficient
- $K_{0,\theta}$: Frequency factor
- $Q_\theta$: Activation energy
- $R$: Gas constant
- $T$: Tempering temperature
- $t$: Tempering time

Similarly, for ε-carbide

$$V_\varepsilon = V_{\varepsilon,max}*(1 - \exp\{-(\beta_\varepsilon)\wedge n_\varepsilon\})*\exp\{-(\beta_\theta)\wedge n_\theta\}$$

$$\beta_\varepsilon(t) = K_{0,\varepsilon} \int \exp(-Q_\varepsilon/(R*T(t))\, dt$$

Here, the JMA equation is multiplied by the exponential term for cementite. This modification considers the decrease in ε-carbide as cementite is formed [10]. The kinetic parameters used for this model are shown in Table 2. The maximum volume fraction of cementite is calculated using Thermo-Calc version 2021b [16].

Table 2 Kinetic parameters. [10]

| $n_\varepsilon$ | $K_{0,\varepsilon}$ | $Q_\varepsilon$ kJ/mol | $n_\theta$ | $K_{0,\theta}$ | $Q_\theta$ kJ/mol |
|---|---|---|---|---|---|
| 0.68 | 1.03*10^15 | 117 | 1.1 | 8*10^14 | 206 |

## 4. Results

### 4.1 SEM and TEM Investigation

SEM analysis was performed for the 2 h and 6 h tempered specimens with a tempering temperature of 600 °C. In each case, 4 to 5 images were evaluated. An output from the SEM investigation and the image after processing with Fiji software is shown in Figure 2. Box plots indicating the area fraction from all the evaluated images are seen in Figure 3.

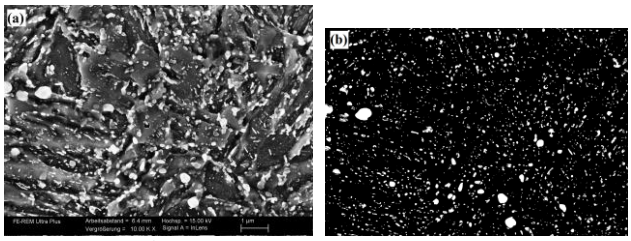

Figure 2 SEM of 2 h, 600 °C tempered specimen. a) SEM image and b) processed image for evaluation.

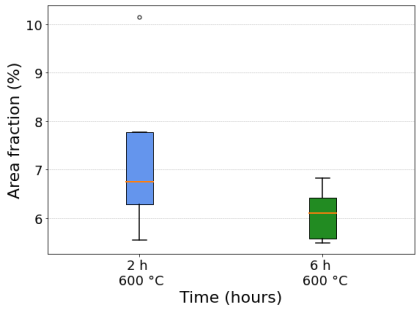

Figure 3 Results from SEM evaluation.

For the tempering temperature of 300 °C and 400 °C, the TEM approach was used. A comparison between SEM and TEM was done with a 2 h, 600 °C tempered specimen. A bright field TEM image along with EDXS and processed image is shown in Figure 4. And the overview of all TEM evaluations is seen in Figure 5.

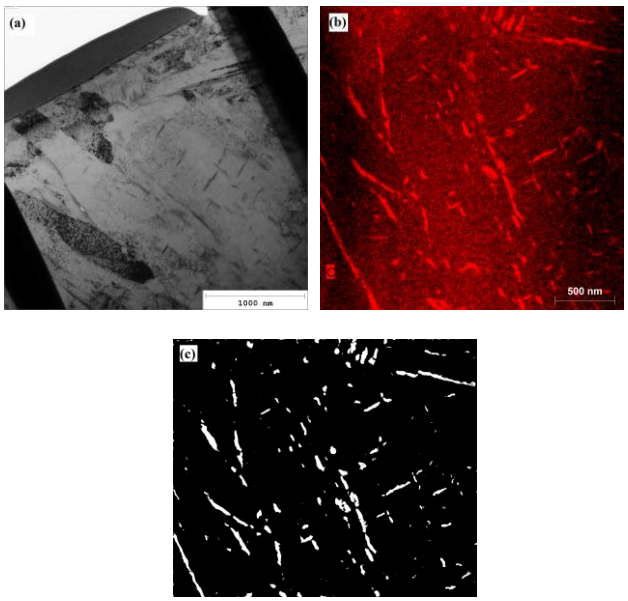


Figure 4 TEM of 6 h, 300 °C tempered specimen. a) TEM bright field image, b) EDXS image and c) processed image for evaluation.

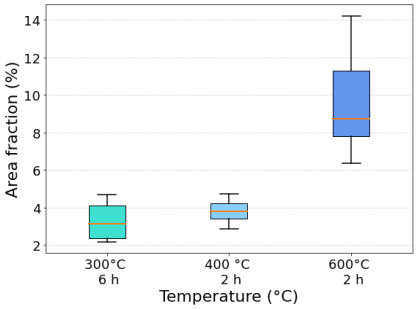


Figure 5 Results from TEM evaluation.

### 4.2 Precipitation Modeling

The chemical composition at every point in the specimen may not be the same as mentioned in Table 1. To account for this variation, C and Cr wt% were varied as per the permissible range mentioned in 50CrMo4 material data sheets. This provides the possible range of variation in the volume fraction of the carbides. Results for $V_{\theta,max}$ from Thermo-Calc was obtained for C wt% (0.46, 0.54) and Cr wt% (0.9, 1.2, 1.31). $V_{\varepsilon,max}$ was set to 0 in this study case to compare the experimental results which were not segregated into different carbides.

The implemented JMA model was run for tempering times of 2 hours and 6 hours. The resulting volume fractions are shown in Figure 6. The precipitation kinetics over the tempering time of 6 hours is seen in Figure 7. The results from the experimental investigations are also plotted in the graph for an overall comparison of both approaches.

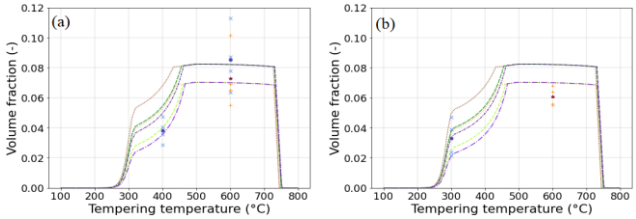


Figure 6 Carbide volume fraction at different tempering temperatures. a) tempered for 2 h , b) tempered for 6 h.

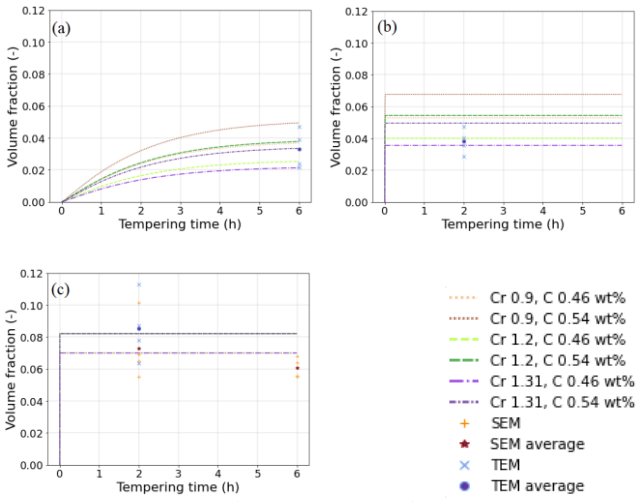


Figure 7 Carbide volume fraction during 6 h of tempering. a) at 300 °C , b) 400 °C and c) 600 °C.

## 5. Discussion

The experimental investigations show needle shaped precipitates at tempering temperatures of 300 °C and 400 °C. At 600 °C, more spherical precipitates are observed. This indicates ε-carbide, cementite at lower temperatures and spheroidization of cementite at higher temperatures. The fraction of carbides tends to increase as the tempering temperature increases from 300 °C to 600 °C. However, at higher tempering temperature, there is a range of overlap with average value showing a decrease from 2 to 6 hours.

In Figure 7a, the modeling results show the kinetics occurring at 300 °C in the duration of 6 h. But, at higher tempering temperatures, the volume fraction obtained at 2 h or 6 h is similar. This is also observed in the volume fraction versus temperature graph, where the major change between 2 and 6 h is seen below 400 °C. In Figure 6 and 7, as the carbon content decreases, the carbide volume fraction also decreases. Chromium content influences the formation of cementite at temperatures of 300 °C and 400 °C. With an increase in chromium a decrease in the volume fraction is observed. However, there is no influence at 600 °C.

The experimental microstructure characterization values are also seen in the modeling plots. It can be seen that in most cases the values fall within the range of the model, or the average values are close to the calculated volume fractions. The results from SEM 6 h, 600 °C tends to show lower than model values.

## 6. Summary

Quenched and tempered martensitic 50CrMo4 steel was the focus material. A deep dive into the precipitation in the specimens during the tempering is obtained via experimental or kinetic modeling.

- SEM and TEM approach enabled experimental microstructure characterization.

- JMA model provided reasonable results
- The fraction of the carbides formed was validated
- Further microstructure characterization can facilitate a better experimental statistics.
- Further parameters like diameter, number density can be checked with further kinetic modelling.

## 7. References


1. B.J. Schäfer, X. Song, P. Sonnweber-Ribic, H. ul Hassan and A. Hartmaier: Metals **9** (2019) 368.
2. V. Jászfi, P. Prevedel, A. Eggbauer, Y. Godai, P. Raninger, D. Mevec, M. Panzenböck and R. Ebner: HTM J. Heat Treatm. Mat. **74** (2019) 366-379.
3. A. Eggbauer, G. Ressel, P. Raninger, P. Prevedel, S. Marsoner and R. Ebner: Metall. Res. Technol. **115** (2018) 407.
4. S.T. Ahn, D.S. Kim and W.J. Nam: J. Mater. Process. Technol. **160** (2005) 54-58.
5. W.J. Nam, D.S. Kim and S.T. Ahn: J. Mater. Sci. **38** (2003) 3611–3617.
6. A. Vieweg, E. Povoden-Karadeniz, G. Ressel, P. Prevedel, T. Wojcik, F. Mendez-Martin, A. Stark, J. Keckes and E. Kozeschnik: Mater. Des. **136** (2017) 214-222.
7. Z. Hou, R.P. Babu, P. Hedström and J. Odqvist: J Mater Sci **53** (2018) 6939–6950.
8. M. Perez, A. Deschamps: Mater. Sci. Eng. A **360** (2003) 214-219.
9. J.D. Robson and H.K.D.H. Bhadeshia: Mater. Sci. Technol **13** (1997) 631-639
10. X. Deng, and D. Ju: Mater. Perform. Charact. **3** (2015) 20130104.
11. Y. Wang, S. Denis, B. Appolaire and P. Archambault: J. Phys. IV **120** (2004) 103-110.
12. A. Deschamps and C.R. Hutchinson: Acta Mater **220 (**2021) 117338.
13. A. Pohjonen, S.R. Babu, V. Visuri: Comput. Mater. Sci. **209** (2022) 111413.
14. M. Graf, M. Kuntz, H. Autenrieth and R. Müller: Appl. Sci. **10** (2020) 5395.
15. J. Schindelin, I. Arganda-Carreras, E. Frise, et al.: Nat Methods **9** (2012) 676–682.
16. J-O Andersson, T. Helander, L. Höglund, P. Shi and B. Sundman: Calphad, **26** (2002) 273-312.